Comparative differences in the atherosclerotic disease burden between the epicardial coronary arteries: quantitative plaque analysis on coronary computed tomography angiography

Bax, A.M.; Rosendael, A.R. van; Ma, X.Y.; Hoogen, I.J. van den; Gianni, U.; Tantawy, S.W.; ... ; PARADIGM Investigators

ESC European Society of Cardiology

European Heart Journal - Cardiovascular Imaging (2021) **22**, 322–330
doi:10.1093/ehjci/jeaa275

Comparative differences in the atherosclerotic disease burden between the epicardial coronary arteries: quantitative plaque analysis on coronary computed tomography angiography

A. Maxim Bax[1], Alexander R. van Rosendael[1,2], Xiaoyue Ma[3], Inge J. van den Hoogen[1,2], Umberto Gianni[1], Sara W. Tantawy[1], Emma J. Hollenberg[1], Daniele Andreini[4], Mouaz H. Al-Mallah[5], Matthew J. Budoff[6], Filippo Cademartiri[7], Kavitha Chinnaiyan[8], Jung Hyun Choi[9], Edoardo Conte[4], Hugo Marques[10], Pedro de Araújo Gonçalves[10,11], Ilan Gottlieb[12], Martin Hadamitzky[13], Jonathon A. Leipsic[14], Erica Maffei[15], Gianluca Pontone[4], Sanghoon Shin[16], Yong-Jin Kim[17], Byoung Kwon Lee[18], Eun Ju Chun[19], Ji Min Sung[20,21], Sang-Eun Lee[16,21], Renu Virmani[22], Habib Samady[23], Peter H. Stone[24], Daniel S. Berman[25], James K. Min[26], Jagat Narula[27], Fay Y. Lin[1], Hyuk-Jae Chang[20,21†], and Leslee J. Shaw[1*†]; for the PARADIGM Investigators[‡]

[1]Department of Radiology, Dalio Institute of Cardiovascular Imaging, New York-Presbyterian Hospital and Weill Cornell Medicine, New York, NY, USA; [2]Department of Cardiology, Leiden University Medical Center, Leiden, The Netherlands; [3]Department of Healthcare Policy and Research, New York-Presbyterian Hospital and the Weill Cornell Medical College, New York, NY, USA; [4]Department of Medicine, Centro Cardiologico Monzino, IRCCS, Milan, Italy; [5]Department of Cardiology, Houston Methodist DeBakey Heart & Vascular Center, Houston Methodist Hospital, Houston, TX, USA; [6]Department of Medicine, Los Angeles Biomedical Research Institute, Torrance, CA, USA; [7]Department of Radiology, Cardiovascular Imaging Center, SDN IRCCS, Naples, Italy; [8]Department of Cardiology, William Beaumont Hospital, Royal Oak, MI, USA; [9]Division of Cardiology, Department of Internal Medicine, Pusan University Hospital, Busan, South Korea; [10]Department of Radiology,UNICA, Unit of Cardiovascular Imaging, Hospital da Luz, Nova Medical School, Lisboa, Portugal; [11]Department of Cardiology, NOVA Medical School, Lisboa, Portugal; [12]Department of Radiology, Casa de Saude São Jose, Rio de Janeiro, Brazil; [13]Department of Radiology and Nuclear Medicine, German Heart Center, Munich, Germany; [14]Department of Medicine and Radiology, University of British Columbia, Vancouver, BC, Canada; [15]Department of Radiology, Area Vasta 1/ASUR Marche, Urbino, Italy; [16]Division of Cardiology, Department of Internal Medicine, Ewha Woman's University Seoul Hospital, Seoul, Korea; [17]Department of Internal Medicine, Seoul National University College of Medicine, Cardiovascular Center, Seoul National University Hospital, Seoul, South Korea; [18]Division of Cardiology, Department of Internal Medicine, Gangnam Severance Hospital, Yonsei University College of Medicine, Seoul, Korea; [19]Department of Radiology, Seoul National University Bundang Hospital, Sungnam, South Korea; [20]Division of Cardiology, Severance Cardiovascular Hospital, Yonsei University College of Medicine, Yonsei University Health System, Seoul, South Korea; [21]Yonsei-Cedars-Sinai Integrative Cardiovascular Imaging Research Center, Yonsei University College of Medicine, Yonsei University Health System, Seoul, South Korea; [22]Department of Pathology, CVPath Institute, Gaithersburg, MD, USA; [23]Division of Cardiology, Emory University School of Medicine, Atlanta, GA, USA; [24]Cardiovascular Division, Department of Medicine, Brigham and Women's Hospital, Harvard Medical School, Boston, MA, USA; [25]Department of Imaging and Medicine, Cedars Sinai Medical Center, Los Angeles, CA, USA; [26]Cleerly, Inc., New York, NY, USA; and [27]Department of Cardiology, Icahn School of Medicine at Mount Sinai, Mount Sinai Heart, Zena and Michael A. Wiener Cardiovascular Institute, and Marie-Josée and Henry R. Kravis Center for Cardiovascular Health, New York, NY, USA

Received 12 May 2020; editorial decision 17 September 2020; accepted 18 September 2020; online publish-ahead-of-print 20 November 2020

Aims Anatomic series commonly report the extent and severity of coronary artery disease (CAD), regardless of location. The aim of this study was to evaluate differences in atherosclerotic plaque burden and composition across the major epicardial coronary arteries.

Methods and results A total of 1271 patients (age 60 ± 9 years; 57% men) with suspected CAD prospectively underwent coronary computed tomography angiography (CCTA). Atherosclerotic plaque volume was quantified with categorization by composition (necrotic core, fibrofatty, fibrous, and calcified) based on Hounsfield Unit density. Per-vessel measures

* Corresponding author. Tel: +1 (929) 304 7734. E-mail: les2035@med.cornell.edu
† These authors serve as co-senior authors of this manuscript.
‡ A full list of PARADIGM investigators is provided in the Supplementary dataonline, Appendix.

were compared using generalized estimating equation models. On CCTA, total plaque volume was lowest in the LCx (10.0 ± 29.4 mm^3), followed by the RCA (32.8 ± 82.7 mm^3; $P < 0.001$), and LAD (58.6 ± 83.3 mm^3; $P < 0.001$), even when correcting for vessel length or volume. The prevalence of ≥2 high-risk plaque features, such as positive remodelling or spotty calcification, occurred less in the LCx (3.8%) when compared with the LAD (21.4%) or RCA (10.9%, $P < 0.001$). In the LCx, the most stenotic lesion was categorized as largely calcified more often than in the RCA and LAD (55.3% vs. 39.4% vs. 32.7%; $P < 0.001$). Median diameter stenosis was also lowest in the LCx (16.2%) and highest in the LAD (21.3%; $P < 0.001$) and located more distal along the LCx when compared with the RCA and LAD ($P < 0.001$).

Conclusion Atherosclerotic plaque, irrespective of vessel volume, varied across the epicardial coronary arteries; with a significantly lower burden and different compositions in the LCx when compared with the LAD and RCA. These volumetric and compositional findings support a diverse milieu for atherosclerotic plaque development and may contribute to a varied acute coronary risk between the major epicardial coronary arteries.

Graphical Abstract

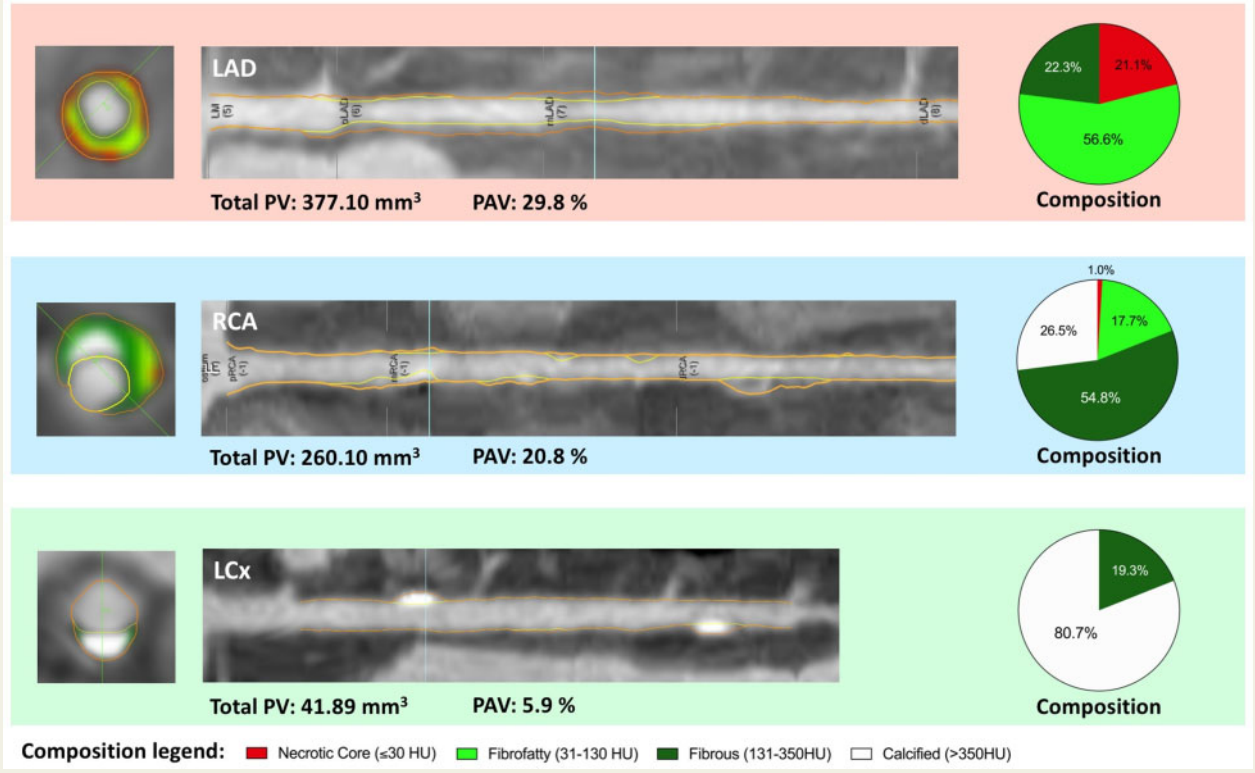

Keywords coronary computed tomography angiography • coronary artery disease • coronary artery plaque composition

Introduction

Atherosclerotic plaque imaging has rapidly advanced from initial studies using invasive techniques, such as intra-vascular ultrasound or optical coherence tomography[1,2] to more recent advancements using coronary computed tomography angiography (CCTA) as a non-invasive alternative for qualitative and quantitative measurement of atherosclerosis.[3–5] Within the field of anatomic imaging, there has been extensive research establishing the prognostic significance and therapeutic benefit from intervention based on the severity and location of obstructive coronary artery disease (CAD).[6–9] Specifically, prior invasive angiographic data revealed that the left circumflex (LCx) coronary artery is more often observed with single when compared with multivessel CAD when compared with that in the left anterior descending (LAD) or right coronary artery (RCA).[10] Moreover, among patients with STEMI, the location of a culprit lesion

is reported less often in the LCx when compared with the LAD or RCA.[11] In stable patients, lower coronary artery calcium scores were also reported in the LCx when compared with the LAD or RCA.[12] These findings in largely smaller cohorts suggest a varied milieu for atherosclerosis development. To date, comprehensive comparisons between the epicardial coronary arteries concerning the presence and severity of coronary atherosclerosis have not been reported.

The Progression of AtheRosclerotic PlAque DetermIned by Computed TomoGraphic Angiography (PARADIGM) registry previously reported on alterations in atherosclerotic plaque with statin therapy.[13] In the current report, we undertook a comparative analysis of differences in the burden and composition of quantitative atherosclerotic plaque by the location of the epicardial coronary artery; primarily comparing the LCx with LAD and RCA. Differences were also compared based on correction for vessel volume, including analysis by the percent atheroma volume (PAV).

Methods

Study design

PARADIGM was a multinational, dynamic observational cohort that prospectively enrolled patients undergoing CCTA between 2003 and 2015.[14] The research protocol was approved by each centre's institutional review board. Details of the PARADIGM registry are found in the report by Lee *et al.*[15]

Patient enrolment

A total of 2252 patients with suspected CAD undergoing CCTA were prospectively enrolled from 13 sites in 7 countries (Brazil, Canada, Germany, Italy, Portugal, South Korea, and the USA).[14] For this analysis, patients that had undergone revascularization (defined as percutaneous coronary intervention and/or coronary artery bypass grafting; $n = 736$) were excluded, as well as patients with missing analysis of ≥1 coronary artery on CCTA ($n = 245$). Thus, the current analysis included 1271 patients ($n = 3813$ vessels).

CCTA acquisition and interpretation

All CCTAs were performed in accordance with the Society of Cardiovascular Computed Tomography guidelines.[16,17] Datasets from each participating site were transferred to a core laboratory for blinded image analysis. Coronary atherosclerosis was evaluated on multiplanar and cross-sectional CCTA images. All computations were performed by level III experienced readers masked to clinical data, using quantitative plaque software (QAngioCT Research Edition v2.1.9.1, Medis Medical Imaging Systems, Leiden, the Netherlands).[18]

All coronary arteries with a diameter ≥2 mm were evaluated, according to the 17-segment American Heart Association model for coronary segment classification.[17] Presence of plaque was defined as any tissue ≥1 mm^2 identified in >2 planes, within or adjacent to the lumen that could be discriminated from surrounding pericardial tissue, epicardial fat, or lumen.[17,19] Quantitative analysis was performed on a per-segment level. To generate vessel length (mm), vessel volume (mm^3), lumen volume (mm^3), and per-vessel plaque volume (mm^3), measurements of all segments of each vessel, including side branches, were summed. PAV was calculated as follows: [(PV/vessel volume) × 100] %. Based on established Hounsfield Unit (HU) ranges, plaque composition was categorized as calcified (>350 HU)[20], fibrous (131–350 HU), and low-density [necrotic core (≤30 HU) and fibrofatty (31–130 HU)][13,20,21] The proportion of total PV of the compositional subtypes was calculated as: subtype % = [(subtype PV/total per-vessel PV) × 100] %.

Furthermore, individual lesions were evaluated for composition (visually classified as calcified, mixed, or non-calcified), diameter stenosis (%), and high-risk plaque (HRP) defined as ≥2 of the following features: low-attenuation plaque, spotty calcification, positive remodelling, or napkin ring sign[19,22] and distance from the ostium to the point of minimal lumen diameter (mm). Low-attenuation plaque was defined as any lesion containing ≥1 voxel(s) with HU ≤30.[19,23] Spotty calcification was defined by the presence of intra-lesional calcification <3 mm.[22,24] A remodelling index was calculated as a maximal lesion vessel area divided by proximal reference vessel area, with positive remodelling defined by a remodelling index ≥1.1.[25] A napkin ring sign was defined cross-sectionally with a central area of low attenuation plaque and a surrounding ring with higher attenuation plaque.

Study endpoints

All analyses were performed on a per-vessel basis. The primary aim of this report was to compare differences in CCTA-derived atherosclerotic plaque volume between the three major epicardial coronary arteries. Secondary endpoints included comparisons by atherosclerotic plaque compositional subgroups and the location of the most stenotic lesion in the coronary artery.

Statistical analysis

Continuous variables are presented as mean ± SD or median with interquartile range (IQR), while categorical variables are presented as absolute numbers and percentages. Differences between categorical variables were compared using a χ^2 or Fisher's exact test. Continuous variables were compared using either a paired test (Friedman test for three-way or a Wilcoxon signed-rank test) or unpaired test (Mann–Whitney *U* test for per-lesion comparison), as appropriate. To account for within patient clustering of data, generalized estimating equations (GEE) models were used, including linear and logistic models. Odds ratios (ORs) and 95% confidence intervals were calculated. When noted, the GEE models included the atherosclerotic cardiovascular disease risk score, as a covariate. Two-tailed *P*-values <0.05 were considered statistically significant. All analyses were performed in SAS version 9.4 (SAS Institute, Inc., Cary, NC, USA) and SPSS Statistics version 25 (IBM Corporation, Armonk, NY, USA).

Results

Baseline characteristics

From 2252 patients enrolled in the PARADIGM registry, 1271 (mean age 60.3 ± 9.3 years; 57% men) were included in the current analysis (*Table 1*). A majority of enrolled patients were symptomatic prior to their CCTA (81%). The overall prevalence of CAD risk factors was 51.8% for hypertension, 37.5% for hyperlipidaemia, 19.8% for diabetes mellitus, and 18.4% for smoking.

Quantitative measurement of atherosclerotic plaque on CCTA

CCTA measurements of the three major coronary arteries are presented in *Table 2*. On average, the LAD was the longest vessel (169.0 ± 57.8 mm), whereas the RCA was the largest vessel in terms of volume (1042.5 ± 604.0 mm^3). The LCx was smaller in terms of vessel length (98.5 ± 43.8 mm) and vessel volume (476 ± 305.9 mm^3) than the LAD and RCA ($P < 0.001$ for both). Total plaque

Table 1 Baseline clinical characteristics of the 1271 enrolled patients

	Descriptive statistics (*N* = 1271)
Age, mean ± SD (years)	60.3 ± 9.3
Male sex (%)	724 (57.0)
BMI, mean ± SD (kg/m^2)	25.3 ± 3.3
ASCVD risk score, median (IQR) (%)	9.3 (4.4-17.6)
Chest pain history (%)	
Asymptomatic[a]	182 (14.3)
Non-cardiac chest pain	115 (9.1)
Atypical chest pain	907 (71.8)
Typical angina	48 (3.8)
CAD risk factors (%)	
Diabetes mellitus	251 (19.8)
Hypertension	655 (51.8)
Hyperlipidaemia	474 (37.5)
Family history of CAD	363 (28.6)
Current smoker	232 (18.4)
Medications (%)	
Aspirin	452 (36.2)
β-Blockers	332 (26.6)
Calcium channel blockers	261 (21.0)
Diuretics	111 (8.9)
RAAS inhibitors	350 (28.1)
Statins	474 (38.9)

[a]Asymptomatics in this registry met clinical indications for CCTA and often were referred for pre-operative risk evaluation, prior stress testing, or had a history of non-cardiac atherosclerosis.
ASCVD risk score, atherosclerotic cardiovascular disease risk score; BMI, body mass index; CAD, coronary artery disease; RAAS inhibitors, renin–angiotensin–aldosterone system inhibitors.

volume was smallest in the LCx (10.0 ± 29.4 mm^3), followed by the RCA (32.8 ± 82.7 mm^3; $P < 0.001$), and LAD (58.6 ± 83.3 mm^3; $P < 0.001$). After correcting for vessel volume, the LCx remained the vessel with the smallest percent atheroma volume (PAV 2.0 ± 5.2%), compared with the LAD (6.4 ± 8.1%; $P < 0.001$) and the RCA (2.8 ± 6.3%; $P < 0.001$). For all compositional subtypes, the LAD contained the highest plaque volume, followed by the RCA and lastly the LCx. Furthermore, the number of lesions differed significantly among the coronary arteries, with the LCx containing fewer lesions (0.42 ± 0.77 per artery; $P < 0.001$) and fewer HRP lesions (0.04 ± 0.20 per artery; $P < 0.001$). The prevalence of ≥2 HRP features was significantly lower in the LCx (3.8%) when compared with the LAD (21.4%) and RCA (10.9%, $P < 0.001$). The same was noted for the individual HRP features, such as spotty calcification ($P < 0.001$) or positive remodelling ($P < 0.001$).

Atherosclerotic plaque composition on CCTA

The prevalence of plaque across the different coronary arteries is presented in *Figure 1A*. The prevalence of any plaque was the lowest in the LCx (29.8%), followed by the RCA (39.8%; $P < 0.001$) and LAD (69.8%; $P < 0.001$). Similarly, the presence of low-density plaque (combining necrotic core and fibrofatty plaque) was lowest in the LCx, followed by RCA and LAD (20.9%, 34.2%, and 64.4%, respectively, $P < 0.001$).

Moreover, both necrotic core (LCx 0.7%; RCA 1.7%; LAD 2.3%, $P < 0.001$) and fibrofatty plaque (LCx 10.3%; RCA 16.6%; LAD 18.9%, $P < 0.001$) comprised the smallest proportion of the total plaque volume in the LCx (*Figure 1B*). The mean proportion of calcified plaque was highest in the LCx (39.4%) when compared with the RCA (31.3%) and LAD (31.2%) ($P < 0.001$), whereas proportions of fibrous plaque were similar in all three vessels.

Comparisons of atherosclerotic plaque using regression modelling

To consider the within patient clustering of vessels, we compared plaque compositional subtypes using a GEE logit model (*Table 3*). The multivariate model included the atherosclerotic cardiovascular disease risk score and vessel length as covariates. The adjusted odds of any plaque classified as necrotic core was 3.5- and 2.8-fold higher in the LAD ($P < 0.001$) and RCA ($P < 0.001$) vs. the LCx. Fibrofatty plaque was also significantly more likely to be present in the LAD (OR 4.1; $P < 0.001$) and RCA (OR 2.3; $P < 0.001$) than in the LCx; while the presence of any fibrous or calcified plaque was similar across the coronary arteries.

In a GEE linear model, the ratio of necrotic core to total vessel plaque volume was nearly two-fold higher in the LAD (ratio: 1.8; $P = 0.001$) and RCA (ratio: 1.7; $P = 0.004$) than in the LCx. Similar observations were made for the ratio of fibrofatty plaque (ratio LAD vs. LCx: 1.8; ratio RCA vs. LCx: 1.6; $P < 0.001$ for both). However, the ratio of calcified plaque to total vessel plaque volume was significantly lower in the LAD (ratio 0.8; $P < 0.001$) and RCA (ratio 0.8; $P < 0.001$) than in the LCx; all comparisons were adjusted for the atherosclerotic cardiovascular disease risk score and statin use. Proportions of fibrous plaque did not differ significantly between the coronary arteries.

Comparisons of CCTA characteristics in the most stenotic lesion

In the LCx, the most stenotic lesion was categorized as largely calcified more so than in the RCA and LAD (55.8% vs. 39.4% vs. 32.7%, respectively; $P < 0.001$; see *Figure 2A*). Diameter stenosis was also lowest in the LCx [16.2% (IQR 9.4–25.1%)], followed by the RCA [19.3% (IQR 10.5–28.4%); $P = 0.017$], and the LAD [21.3% (IQR 12.5–31.4%); $P < 0.001$; see *Figure 2B*]. Distance from the ostium to the most severe stenosis was similar in the LCx and RCA [33.6 mm (IQR 22.4–47.3 mm) vs. 33.8 mm (IQR 21.1–64.2 mm); $P = 0.260$] and was shorter in the LAD [28.5 mm (IQR 18.0–38.6 mm); $P < 0.001$]. As such, the most stenotic lesion was more often located more distal in the LCx, occurring at 34.4% of the length of the vessel (as measured from the ostium), when compared with 21.8% for the RCA ($P < 0.001$) and 17.0% for the LAD ($P < 0.001$).

Discussion

While there is abundant evidence regarding the prevalence and risk associated with various stenosis and plaque findings on CCTA, there

Table 2 Comparison of atherosclerotic plaque volume and composition between the major epicardial coronary arteries

	Mean ± SD or %			*P*-value		
Vessel analysis	**LAD (*N* = 1271)**	**RCA (*N* = 1271)**	**LCx (*N* = 1271)**	**Overall[a]**	**LCx vs. LAD[b]**	**LCx vs. RCA[b]**
Vessel length (mm)	169.0 ± 57.8	154.1 ± 51.5	98.5 ± 43.8	<0.001	<0.001	<0.001
Vessel volume (mm^3)	900.4 ± 401.2	1042.5 ± 604.0	476.3 ± 305.9	<0.001	<0.001	<0.001
Lumen volume (mm^3)	841.7 ± 381.6	1009.8 ± 586.8	466.3 ± 301.3	<0.001	<0.001	<0.001
Plaque volume (mm^3)	58.6 ± 83.3	32.8 ± 82.7	10.0 ± 29.4	<0.001	<0.001	<0.001
Necrotic core (≤30 HU)	1.6 ± 5.3	0.6 ± 3.3	0.1 ± 1.2	<0.001	<0.001	<0.001
Fibrofatty (31–130 HU)	12.0 ± 24.2	5.8 ± 18.3	1.1 ± 5.2	<0.001	<0.001	<0.001
Fibrous (131–350 HU)	25.3 ± 36.8	15.8 ± 40.9	4.7 ± 14.6	<0.001	<0.001	<0.001
Calcified (>350 HU)	19.7 ± 41.2	10.7 ± 37.4	4.1 ± 14.4	<0.001	<0.001	<0.001
PAV (%)	6.4 ± 8.1	2.8 ± 6.3	2.0 ± 5.2	<0.001	<0.001	<0.001
Number of lesions per vessel	1.10 ± 0.99	0.72 ± 1.15	0.42 ± 0.77	<0.001	<0.001	<0.001
≥2 HRP features (%)	21.3	10.9	3.8	<0.001		
Low-attenuation plaque (%)	15.1	7.2	1.8	<0.001		
Spotty calcification (%)	13.8	6.3	2.9	<0.001		
Positive remodelling (%)	56.1	33.0	22.7	<0.001		
Napkin-ring sign (%)	0.5	0.2	0.0	0.002		
Number of HRP lesions per vessel	0.21 ± 0.43	0.11 ± 0.37	0.04 ± 0.20	<0.001	<0.001	<0.001

HRP, high-risk plaque; HU, Hounsfield Units; LAD, left anterior descending; LCx, left circumflex; PAV, percent atheroma volume; RCA, right coronary artery.
[a]Friedman test.
[b]Wilcoxon signed-rank test.

has been little attention to differences in the burden and composition of atherosclerotic plaque between the major epicardial coronary arteries. Our results revealed that the LCx contained a lower burden of plaque, even when correcting for vessel volume ($P < 0.001$). Compared with the other coronary arteries, the LCx also showed a different compositional structure of plaque, containing a larger proportion of calcified plaque along with smaller proportions of low-density plaque. Moreover, low-density plaque, which is often associated with higher risk for future coronary events, was less often present in the LCx when compared with the LAD and RCA. These findings have implications for disease detection and support the variable findings reported for ischaemia provocation across the epicardial coronary tree. Importantly, the occurrence of more distal disease that is more calcified with a lower plaque burden and fewer high-risk plaque features is congruent with more stable atherosclerosis and a reduced likelihood for future ischaemic events.

Jeopardized myocardium and risk across the epicardial coronary arteries

Risk assessment of patients based on angiographic findings have been previously reported. Several risk scores, such as the Duke CAD prognostic index[6] or SYNTAX score,[26] uniquely identify risk associated with an LAD stenosis, especially in a proximal location. This higher risk status relates to the sizeable proportion of jeopardized myocardium subtended by the LAD.[27] Additionally, the prevalence of culprit lesions when examined in STEMI series is notably less in the LCx. Additional research findings also reveal that lateral electrocardiographic leads or LCx stress imaging vascular territory abnormalities have a significantly lower diagnostic accuracy; albeit also impacted upon by suboptimal localization and visualization.

The evidence is far from robust and for most of the analyses ranking disease burden and risk, the LCx has historically been the focus of fewer and smaller patient series. Several studies including patients with suspected CAD have shown a lower prevalence of significant stenosis in the LCx.[28,29] The absence of coronary stenosis occurs more often in the LCx (44%) when compared with the LAD (14%); in addition, a more severe stenosis (≥50%) is more often observed in the LAD when compared with the RCA and LCx.[28] In addition, Kang *et al.*[29] examined patients with significant stenosis on invasive coronary angiography, revealing the lowest prevalence of obstructive CAD in the LCx. These data support the improved survival reported for patients with one-vessel obstructive CAD in the LCx when compared with that of patients with isolated obstructive CAD in the LAD or RCA.[30]

Potential mechanisms influencing atherosclerotic plaque between the epicardial coronary arteries

Our analysis reveals a lower burden of atherosclerosis in the LCx on CCTA, suggesting the possibility of a more stable and less turbulent atherosclerotic milieu in that vessel. These data are supported by prior evidence noting higher fractional flow reserve measures in the LCx when compared with the LAD, despite equivalent percent stenosis.[31] It is purported that local haemodynamic forces play an important role in the development of atherosclerosis in the coronary arteries.[32,33] Wall shear stress, the drag force of circulating blood onto the endothelial surface of the artery, is not uniformly distributed across the coronary arteries, with areas of low wall shear stress

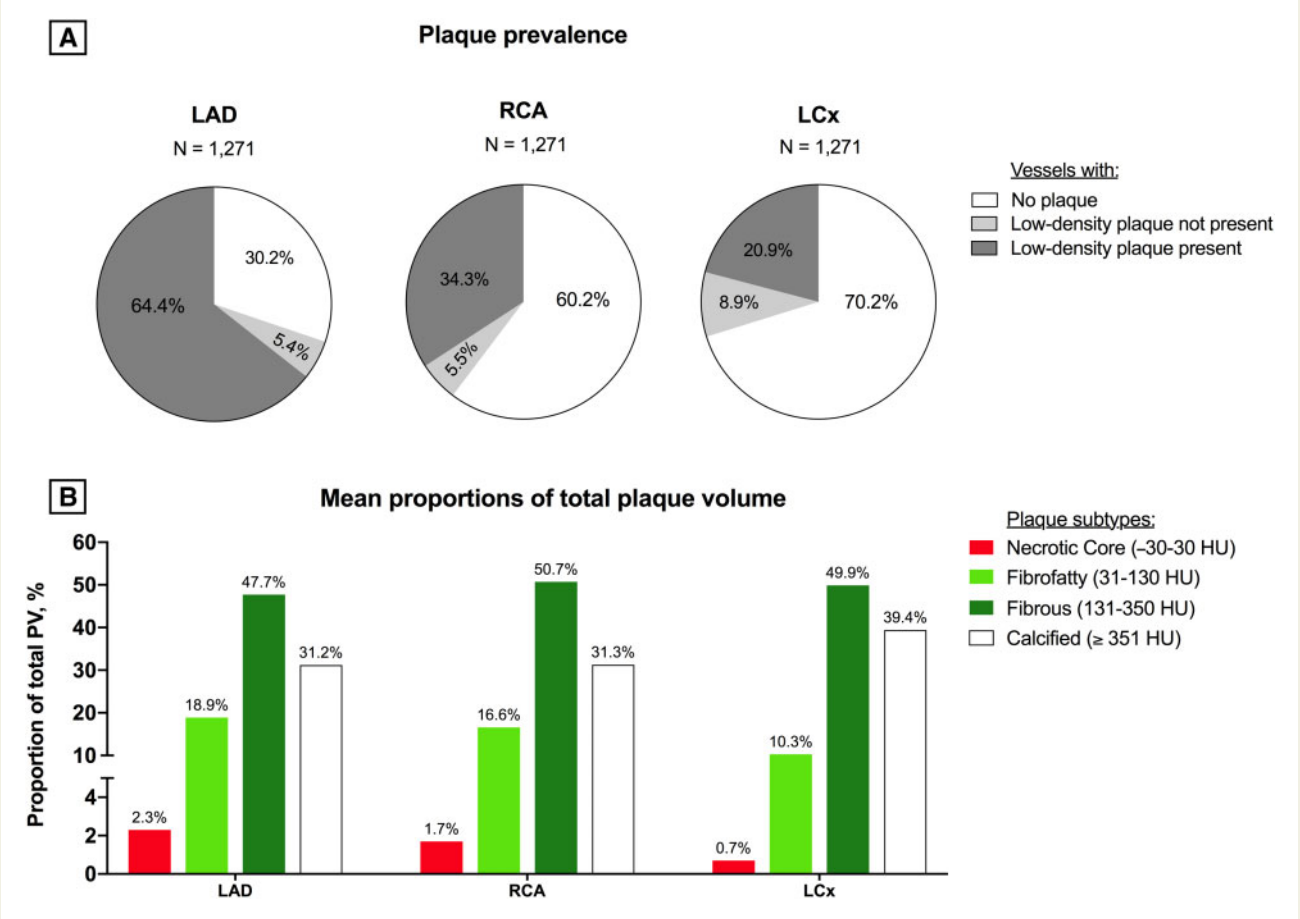

Figure 1 Overview of plaque composition findings per-vessel. (*A*) The prevalence of low-density (necrotic core and fibrofatty) plaque across the coronary arteries is presented in pie charts. Low-density plaque was less prevalent in the LCx ($P < 0.001$). (*B*) Mean proportions of total plaque volume made up by compositional subtypes are presented in bar charts. In the LCx, necrotic core (≤30 HU) and fibrofatty plaque (31–130 HU) comprised less of the total plaque volume, whereas calcified plaque (>350 HU) made up larger proportions, when compared with the LAD and RCA.

Table 3 Comparison of the odds of atherosclerotic disease prevalence and the ratio of plaque composition subgroups in the LAD and RCA vs. the LCx

	Adjusted odds ratio (aOR) and 95% confidence interval (CI)			
	LAD vs. LCx		RCA vs. LCx	
	aOR of any plaque (95% CI)[a]	*P*-value	aOR of any plaque (95% CI)[a]	*P*-value
Necrotic core	3.5 (2.6–4.6)	<0.001	2.8 (2.0–3.9)	<0.001
Fibrofatty	4.1 (2.8–6.0)	<0.001	2.3 (1.6–3.3)	<0.001
Calcified	1.2 (0.8–1.9)	0.379	0.8 (0.5–1.2)	0.280
	Ratio of composition type volume/total per-vessel plaque volume			
	LAD vs. LCx		RCA vs. LCx	
	Ratio (95% CI)[b]	*P*-value	Ratio (95% CI)[b]	*P*-value
Necrotic core	1.8 (1.3–2.6)	0.001	1.7 (1.2–2.4)	0.004
Fibrofatty	1.8 (1.5–2.2)	<0.001	1.6 (1.2–2.0)	<0.001
Calcified	0.8 (0.7–0.9)	<0.001	0.8 (0.6–0.9)	<0.001

LAD, left anterior descending; LCx, left circumflex; RCA, right coronary artery.
[a]The logit GEE model calculated the aOR controlling for vessel length, atherosclerotic cardiovascular disease risk score, and statin use as covariates.
[b]Calculated from a linear GEE-model, adjusted for atherosclerotic cardiovascular disease risk score, and statin use. Ratios were calculated by dividing the proportions of compositional subtypes, in two vessels. E.g. the ratio for necrotic core in the LAD vs. LCx = ([necrotic core volume/plaque volume] $_{LAD}$ / [necrotic core volume/plaque volume] $_{LCx}$).

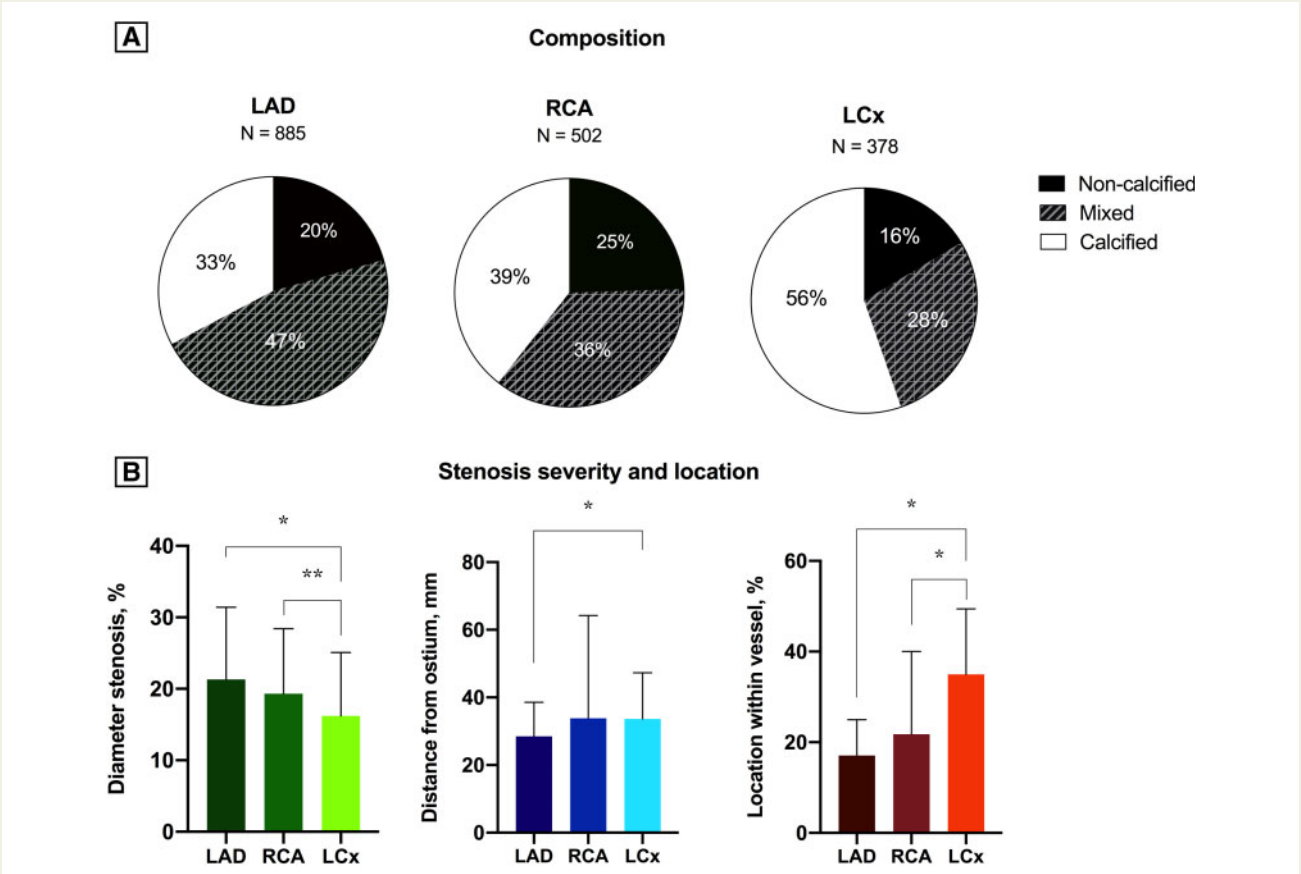

Figure 2 Characteristics of the worst stenosis across the coronary arteries. (*A*) Composition of the most stenotic lesion in the coronary artery, based on visual analysis, is presented in pie charts. Most stenotic lesions were classified as calcified more often in the LCx when compared with the LAD or RCA. (*B*) Left to right: diameter stenosis (%), distance from the aortic ostium to point of minimal lumen diameter (mm), and location within the coronary vessel (% of length from the ostium). Lesions were less stenotic and located more distal in the LCx compared with the other coronary arteries. Bars represent medians with IQR and were compared using the Mann–Whitney *U* test. *$P < 0.001$; **$P < 0.05$.

located at the main bifurcation of the left coronary artery and its proximal segments,[34–36] especially when the bifurcation angle is more obtuse.[37] The strong correlation between low wall shear stress and atherogenesis has been confirmed,[38–40] potentially explaining our observed differences in atherosclerotic burden between the different coronary arteries.

Additionally, Wasilewski *et al.*[41] hypothesized that the squeezing of the septal perforators of the LAD during systole could result in retrograde flow in the LAD segment proximal to the septal perforators, leading to disrupted flow and consequently to the formation of atherosclerosis. Although these studies are not definitive, they mirror our observed findings of a lower burden and severity of coronary atherosclerosis in the LCx when compared with the LAD and RCA.

Study limitations

The current study has several limitations. The design was that of an observational registry, which lends itself to selection and other biases. Furthermore, plaque quantification software used herein is semi-automated, requires tracing of centrelines in the coronary arteries, and is time consuming. Side branches, especially the obtuse marginal side branches of the LCx, were often tortuous and therefore more complex to trace by hand to their full length. This may lead to variable measurement issues across the coronary arteries.

Conclusions

Our findings revealed that atherosclerotic burden differs among the coronary arteries, with the LCx being the vessel with the lowest plaque burden. Moreover, varied admixtures were noted with more calcified plaque in the LCx when compared with the LAD and RCA, potentially suggesting more stabilized CAD. In addition, low-density plaque (necrotic core and fibrofatty plaque) was more prevalent in the LAD and RCA (when compared with the LCx). This research provides further insight into the possible explanation for the uneven distribution of observed culprit lesions among the coronary arteries and the varied prognosis reported in the literature.

Supplementary data

Supplementary data are available at *European Heart Journal - Cardiovascular Imaging* online.

Acknowledgements

The authors acknowledge the PARADIGM investigators for their continued collaboration.

Data availability

The data underlying this article cannot be shared publicly due to the patients' privacy. Data may be available upon reasonable request to the corresponding author, pending investigator approval of the study hypothesis and presence of an institutional data use agreement.

Funding

This work was supported by the Leading Foreign Research Institute Recruitment Program through the National Research Foundation funded by the Ministry of Science and Information and Communications Technology of Korea (Grant no. 2012027176). Additional funding was provided by a gift from the Dalio Foundation (New York, NY) and the Michael Wolk Foundation (New York, NY).

Conflict of interest: K.C. is a non-compensated medical advisory board member of Heartflow Inc. J.K.M. has equity interest and is an employee of Cleerly, Inc. H.S. serves on the scientific advisory board of Phillips, has equity interest in Covanos, Inc., and has research grants from Medtronic, Abbott Vascular, and Phillips. L.J.S. serves on the scientific advisory board for Covanos, Inc. All other authors report no conflict of interest.

References

1. Nicholls SJ, Tuzcu EM, Brennan DM, Tardif JC, Nissen SE. Cholesteryl ester transfer protein inhibition, high-density lipoprotein raising, and progression of coronary atherosclerosis: insights from ILLUSTRATE (Investigation of Lipid Level Management Using Coronary Ultrasound to Assess Reduction of Atherosclerosis by CETP Inhibition and HDL Elevation). *Circulation* 2008;**118**:2506–14.
2. Nicholls SJ, Tuzcu EM, Wolski K, Bayturan O, Lavoie A, Uno K *et al.* Lowering the triglyceride/high-density lipoprotein cholesterol ratio is associated with the beneficial impact of pioglitazone on progression of coronary atherosclerosis in diabetic patients: insights from the PERISCOPE (Pioglitazone Effect on Regression of Intravascular Sonographic Coronary Obstruction Prospective Evaluation) study. *J Am Coll Cardiol* 2011;**57**:153–9.
3. Boogers MJ, Broersen A, van Velzen JE, de Graaf FR, El-Naggar HM, Kitslaar PH *et al.* Automated quantification of coronary plaque with computed tomography: comparison with intravascular ultrasound using a dedicated registration algorithm for fusion-based quantification. *Eur Heart J* 2012;**33**:1007–16.
4. de Graaf MA, Broersen A, Kitslaar PH, Roos CJ, Dijkstra J, Lelieveldt BPF *et al.* Automatic quantification and characterization of coronary atherosclerosis with computed tomography coronary angiography: cross-correlation with intravascular ultrasound virtual histology. *Int J Cardiovasc Imaging* 2013;**29**:1177–90.
5. Williams MC, Kwiecinski J, Doris M, McElhinney P, D'Souza MS, Cadet S *et al.* Low-attenuation noncalcified plaque on coronary computed tomography angiography predicts myocardial infarction: results from the multicenter SCOT-HEART Trial (Scottish Computed Tomography of the HEART. *Circulation* 2020;**141**:1452–62.
6. Mark DB, Nelson CL, Califf RM, Harrell FE Jr, Lee KL, Jones RH *et al.* Continuing evolution of therapy for coronary artery disease. Initial results from the era of coronary angioplasty. *Circulation* 1994;**89**:2015–25.
7. Min JK, Shaw LJ, Devereux RB, Okin PM, Weinsaft JW, Russo DJ *et al.* Prognostic value of multidetector coronary computed tomographic angiography for prediction of all-cause mortality. *J Am Coll Cardiol* 2007;**50**:1161–70.
8. van Rosendael AR, Shaw LJ, Xie JX, Dimitriu-Leen AC, Smit JM, Scholte AJ *et al.* Superior risk stratification with coronary computed tomography angiography using a comprehensive atherosclerotic risk score. *JACC Cardiovasc Imaging* 2019;**12**:1987–97.
9. Andreini D, Pontone G, Mushtaq S, Gransar H, Conte E, Bartorelli AL *et al.* Long-term prognostic impact of CT-Leaman score in patients with non-obstructive CAD: results from the COronary CT Angiography EvaluatioN For Clinical Outcomes InteRnational Multicenter (CONFIRM) study. *Int J Cardiol* 2017;**231**:18–25.
10. Badings EA, Hermanides RS, The SHK, Dambrink JE, Rasoul S, van Wijngaarden J *et al.* Comparison of outcomes and intervention among patients with non-ST-segment elevation acute myocardial infarction of those with a left circumflex versus those with a non-left circumflex-related coronary artery (From the ELISA-3 Trial). *Am J Cardiol* 2018;**121**:1123–8.
11. Antoni ML, Yiu KH, Atary JZ, Delgado V, Holman ER, van der Wall EE *et al.* Distribution of culprit lesions in patients with ST-segment elevation acute myocardial infarction treated with primary percutaneous coronary intervention. *Coron Artery Dis* 2011;**22**:533–6.
12. Lai HM, Holtzman D, Aronow WS, DeLuca AJ, Ahn D, Matayev S *et al.* Association of coronary artery calcium with severity of myocardial ischemia in left anterior descending, left circumflex, and right coronary artery territories. *Clin Cardiol* 2012;**35**:61–3.
13. Lee SE, Chang HJ, Sung JM, Park HB, Heo R, Rizvi A *et al.* Effects of statins on coronary atherosclerotic plaques: the PARADIGM Study. *JACC Cardiovasc Imaging* 2018;**11**:1475–84.
14. Lee SE, Chang HJ, Rizvi A, Hadamitzky M, Kim YJ, Conte E *et al.* Rationale and design of the Progression of AtheRosclerotic PlAque DetermIned by Computed TomoGraphic Angiography IMaging (PARADIGM) registry: a comprehensive exploration of plaque progression and its impact on clinical outcomes from a multicenter serial coronary computed tomographic angiography study. *Am Heart J* 2016;**182**:72–9.
15. Lee SE, Sung JM, Andreini D, Al-Mallah MH, Budoff MJ, Cademartiri F *et al.* Differences in progression to obstructive lesions per high-risk plaque features and plaque volumes with CCTA. *JACC Cardiovasc Imaging* 2020;**13**:1409–17.
16. Abbara S, Blanke P, Maroules CD, Cheezum M, Choi AD, Han BK *et al.* SCCT guidelines for the performance and acquisition of coronary computed tomographic angiography: a report of the society of Cardiovascular Computed Tomography Guidelines Committee: endorsed by the North American Society for Cardiovascular Imaging (NASCI). *J Cardiovasc Comput Tomogr* 2016;**10**:435–49.
17. Leipsic J, Abbara S, Achenbach S, Cury R, Earls JP, Mancini GJ *et al.* SCCT guidelines for the interpretation and reporting of coronary CT angiography: a report of the Society of Cardiovascular Computed Tomography Guidelines Committee. *J Cardiovasc Comput Tomogr* 2014;**8**:342–58.
18. Park HB, Lee BK, Shin S, Heo R, Arsanjani R, Kitslaar PH *et al.* Clinical feasibility of 3D automated coronary atherosclerotic plaque quantification algorithm on coronary computed tomography angiography: comparison with intravascular ultrasound. *Eur Radiol* 2015;**25**:3073–83.
19. Motoyama S, Ito H, Sarai M, Kondo T, Kawai H, Nagahara Y *et al.* Plaque characterization by coronary computed tomography angiography and the likelihood of acute coronary events in mid-term follow-up. *J Am Coll Cardiol* 2015;**66**:337–46.
20. van Rosendael AR, Narula J, Lin FY, van den Hoogen IJ, Gianni U, Al Hussein Alawamlh O *et al.* Association of high-density calcified 1K plaque with risk of acute coronary syndrome. *JAMA Cardiol* 2020;**5**:282.
21. Chang HJ, Lin FY, Lee SE, Andreini D, Bax J, Cademartiri F *et al.* Coronary atherosclerotic precursors of acute coronary syndromes. *J Am Coll Cardiol* 2018;**71**:2511–22.
22. Puchner SB, Liu T, Mayrhofer T, Truong QA, Lee H, Fleg JL *et al.* High-risk plaque detected on coronary CT angiography predicts acute coronary syndromes independent of significant stenosis in acute chest pain: results from the ROMICAT-II trial. *J Am Coll Cardiol* 2014;**64**:684–92.
23. Achenbach S, Moselewski F, Ropers D, Ferencik M, Hoffman U, MacNeill B *et al.* Detection of calcified and noncalcified coronary atherosclerotic plaque by contrast-enhanced, submillimeter multidetector spiral computed tomography: a segment-based comparison with intravascular ultrasound. *Circulation* 2004;**109**:14–7.
24. Motoyama S, Kondo T, Sarai M, Sugiura A, Harigaya H, Sato T *et al.* Multislice computed tomographic characteristics of coronary lesions in acute coronary syndromes. *J Am Coll Cardiol* 2007;**50**:319–26.
25. Hoffmann U, Moselewski F, Nieman K, Jang IK, Ferencik M, Rahman AM *et al.* Noninvasive assessment of plaque morphology and composition in culprit and stable lesions in acute coronary syndrome and stable lesions in stable angina by multidetector computed tomography. *J Am Coll Cardiol* 2006;**47**:1655–62.
26. Sianos G, Morel MA, Kappetein AP, Morice MC, Colombo A, Dawkins K *et al.* The SYNTAX Score: an angiographic tool grading the complexity of coronary artery disease. *EuroIntervention* 2005;**1**:219–27.
27. Gziut AI. Comparative analysis of atherosclerotic plaque distribution in the left main coronary artery and proximal segments of left anterior descending and left circumflex arteries in patients qualified for percutaneous coronary angioplasty. *Ann Acad Med Stetin* 2006;**52**:51–62; discussion 62–3.

28. Cami E, Tagami T, Raff G, Fonte TA, Renard B, Gallagher MJ *et al.* Assessment of lesion-specific ischemia using fractional flow reserve (FFR) profiles derived from coronary computed tomography angiography (FFRCT) and invasive pressure measurements (FFRINV): importance of the site of measurement and implications for patient referral for invasive coronary angiography and percutaneous coronary intervention. *J Cardiovasc Comput Tomogr* 2018;**12**:480–92.
29. Kang J, Chun EJ, Park HJ, Cho YS, Park JJ, Kang SH *et al.* Clinical and computed tomography angiographic predictors of coronary lesions that later progressed to chronic total occlusion. *JACC Cardiovasc Imaging* 2019;**12**:2196–206.
30. Califf RM, Tomabechi Y, Lee KL, Phillips H, Pryor DB, Harrell FE Jr *et al.* Outcome in one-vessel coronary artery disease. *Circulation* 1983;**67**:283–90.
31. Harle T, Meyer S, Bojara W, Vahldiek F, Elsasser A. Intracoronary pressure measurement differences between anterior and posterior coronary territories. *Herz* 2017;**42**:395–402.
32. Malek AM, Alper SL, Izumo S. Hemodynamic shear stress and its role in atherosclerosis. *JAMA* 1999;**282**:2035–42.
33. Chien S. Mechanotransduction and endothelial cell homeostasis: the wisdom of the cell. *Am J Physiol Heart Circ Physiol* 2007;**292**:H1209–24.
34. Tarbell JM. Shear stress and the endothelial transport barrier. *Cardiovasc Res* 2010;**87**:320–30.
35. Qi YX, Qu MJ, Long DK, Liu B, Yao QP, Chien S *et al.* Rho-GDP dissociation inhibitor alpha downregulated by low shear stress promotes vascular smooth muscle cell migration and apoptosis: a proteomic analysis. *Cardiovasc Res* 2008;**80**:114–22.
36. Nordgaard H, Swillens A, Nordhaug D, Kirkeby-Garstad I, van Loo D, Vitale N *et al.* Impact of competitive flow on wall shear stress in coronary surgery: computational fluid dynamics of a LIMA-LAD model. *Cardiovasc Res* 2010;**88**:512–9.
37. Chaichana T, Sun Z, Jewkes J. Computation of hemodynamics in the left coronary artery with variable angulations. *J Biomech* 2011;**44**:1869–78.
38. Soulis JV, Farmakis TM, Giannoglou GD, Louridas GE. Wall shear stress in normal left coronary artery tree. *J Biomech* 2006;**39**:742–9.
39. Katritsis D, Kaiktsis L, Chaniotis A, Pantos J, Efstathopoulos EP, Marmarelis V. Wall shear stress: theoretical considerations and methods of measurement. *Prog Cardiovasc Dis* 2007;**49**:307–29.
40. Slager CJ, Wentzel JJ, Gijsen FJ, Schuurbiers JCH, van der Wal AC, van der Steen AFW *et al.* The role of shear stress in the generation of rupture-prone vulnerable plaques. *Nat Rev Cardiol* 2005;**2**:401–7.
41. Wasilewski J, Niedziela J, Osadnik T, Duszańska A, Sraga W, Desperak P *et al.* Predominant location of coronary artery atherosclerosis in the left anterior descending artery. The impact of septal perforators and the myocardial bridging effect. *Kardiochir Torakochirurgia Pol* 2015;**12**:379–85.